Thickness Dependence of Laser Damage in Silicon Thin Films

Prachi Venkat* and Tomohito Otobe

Kansai Institute for Photon Science, National Institutes for Quantum Science and Technology, Kyoto 619-0215, Japan
**Corresponding author's e-mail: venkat.prachi@qst.go.jp*

We have investigated the interaction of intense laser pulses with silicon film using the one-dimensional Three-Temperature Model previously presented by Venkat and Otobe (Applied Physics Express, 15(4), 041008 (2022)). Our study focuses on how the excitation process in thin films, ranging from tens of nanometers to a few microns, is affected by the interference of the laser field at a wavelength of 775 nm. Our findings show that when the thickness of the film is less than 1.5 μm, the damage thresholds exhibit oscillations due to the interference of the laser field over a period of 100 nm, which is equivalent to half the wavelength in silicon. We also observe that the thermal damage threshold of the rear surface and inside film is lower than that of the front surface when the thickness is less than 0.3 μm and 0.5 μm, respectively. These results emphasize the significance of the size effect in the laser processing of silicon and have important implications for the optimization of the laser processing techniques of silicon.
DOI: 10.2961/jlmn.2023.03.2013
Keywords: laser processing, laser damage, silicon, numerical simulation, semiconductor, electron dynamics, three-temperature model

1. Introduction

Laser processing studies of semiconductors like silicon are crucial for practical applications in the field of nano-fabrication. Interaction of intense, femtosecond pulses with a target can provide a high-resolution energy transfer with minimum damage to the surrounding area. Laser excitation of semiconductors involves complex physics of photo-absorption, impact ionization, recombination, and re-distribution of energy. It is the dynamics of the interaction that leads to permanent structural changes through thermal and non-thermal effects. Various processes leading to damage in silicon film have been explored in experimental studies [1-4]. The effect of laser parameters such as the wavelength and pulse duration can also affect the threshold fluence for causing damage in silicon [4,5].

To understand the physics of the interaction and the effect of various parameters, numerical modeling is a useful tool. It allows us to study the dynamics of laser excitation in silicon in detail [6-9]. The onset and nature of damage can be better understood by taking into account all the processes occurring within the lattice and their respective time frames. Theoretical modeling of laser excitation in silicon usually involves the use of Two-Temperature Model (TTM), which has been a widely implemented approach to study the evolution of electron and lattice dynamics during laser excitation. TTM was initially developed to study the dynamics in metals [10] and then extended to study excitation in semiconductors [6,7]. Recently, a self-consistent density-dependent TTM (nTTM) has been implemented to study the evolution of carrier and lattice dynamics in semiconductors [9]. The dynamics following the laser excitation involve a progression of electron-hole-phonon interaction and relaxation. The electron and hole quasi-temperatures are separated in pico-seconds [11]. Electron-hole scattering frequency decreases significantly with the increase in electron temperature [12]. The calculations presented using first-principles numerical simulation show that electron and hole energies evolve differently, depending on the band structure [13]. The energy difference between electrons and holes suggests that quasi-temperatures are different in the conduction band (CB) and valence band (VB) [13]. These studies imply that we need to study the evolution of the electron and hole energies separately in order to understand the electron dynamics and damage processes in semiconductors and dielectrics. A similar study has been presented by Silaeva *et al.* [14] in order to study laser-assisted atom probe tomography. In our previous work, we developed a modified nTTM treating the evolution of quasi-temperatures in CB, VB and lattice (3TM). We found that 3TM shows reasonable agreement for various experimental results [15,16].

The effect of target structure on the dynamics during laser processing can also be significant, depending on the applications. One of the most important applications is the effect of plasmons on the surface in laser-induced periodic surface structures (LIPSS) [17,18]. One of the simplest structures is the thin film, which also affects the LIPSS formation [19]. The non-linear dynamics in silicon thin-film significantly depend on the thickness [20]. In case of a silicon film with thickness less than the penetration depth of the pulse, reflection from the rear surface of the film may interfere with the field within the film, altering the effective pulse intensity and thus, the dynamics. In the case of silicon films of nano-scale thickness, a lower damage threshold may be observed inside the film and on the rear-surface as compared to the front surface of the film.

In this work, we study the thickness dependence of the laser damage threshold of silicon thin-films by employing 3TM with Maxwell's equations. The paper is organized as follows: Section 2 contains the computational details of the one-dimensional 3TM, section 3 consists of the results and

analysis for thickness dependence of damage threshold, and section 4 summarizes the study.

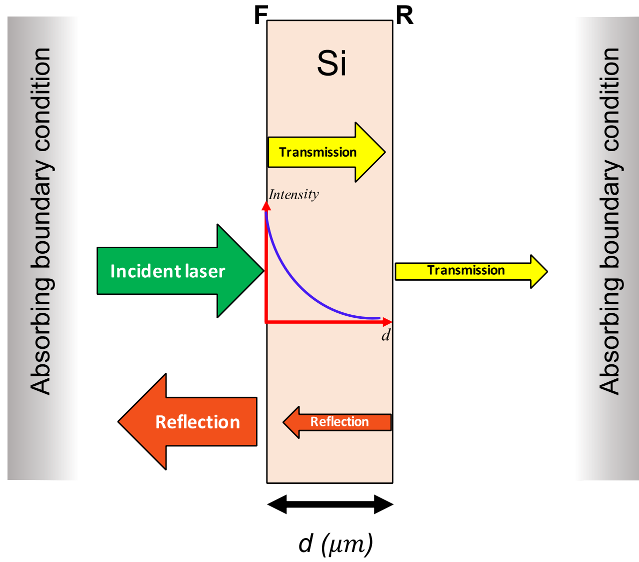

Fig. 1 Schematic representation of laser propagation in a silicon film. As the thickness '*d*' decreases, the interference of the transmitted and reflected field becomes significant.

2. Computational details

Laser irradiation of the silicon target leads to excitation of the electrons from VB to CB, followed by recombination and transfer of energy from the carriers to the lattice, ultimately leading to thermal equilibrium. Single and two-photon absorption, impact ionization and Auger recombination occur during laser excitation of silicon and affect the temporal evolution of transient carrier densities and energy flow in the system. Electron-phonon interaction is responsible for the re-distribution of energy within the carrier and lattice sub-systems.

The present model is similar to nTTM [9], with some crucial changes. The system considers electrons, holes and the lattice as separate sub-systems. Temperatures of the electron, hole and lattice sub-systems also evolve separately through Eq. 3 and 4. The effect of dynamics on the optical properties of silicon is considered. The effect of band gap re-normalization is considered while calculating the dielectric function and single- and two-photon absorption coefficients [21]. The laser field is modeled using the Finite Difference Time Domain (FDTD) method. The model is detailed in Ref. [15].

The electron and hole densities are calculated separately through Eq. 1, where n_e and n_h are calculated as:

$$\frac{\partial n_{e(h)}}{\partial t} = \frac{\alpha I}{\hbar\omega_0} + \frac{\beta I^2}{2\hbar\omega_0} - \gamma_e n_e n_e n_h - \gamma_h n_h n_h n_e + \frac{1}{2}(\theta_e n_e + \theta_h n_h) + \nabla D_{e(h)} \cdot \vec{J}_{e(h)} + D_{e(h)} \nabla \cdot \vec{J}_{e(h)} - (+) n_{e(h)} \nabla \mu_{e(h)} \cdot \vec{F} - (+) \mu_{e(h)} \nabla n_{e(h)} \cdot \vec{F} - (+) \mu_{e(h)} n_{e(h)} \nabla \cdot \vec{F} \quad (1)$$

where ω_0 is the laser frequency and α is the single photon absorption coefficient for a transition from VB to CB [22]. β is the two-photon absorption coefficient for which we use the DFT calculation when $2\hbar\omega_0 > E_0$ [23], where E_0 is the optical gap. Around the band gap energy, we employ interpolation to the model described in Ref. [24-26]. $\gamma_{e(h)}$ is the Auger re-combination coefficient [14] and $\theta_{e(h)}$ is the impact ionization coefficient [9]. Equation 1 also includes the effect of spatial charge distribution and the associated electric field, and $J_{e(h)}$, $D_{e(h)}$ and $\vec{F}$ are the charge current, diffusion coefficient and the electric field induced by the electron-hole separation, respectively [15].

The total dielectric function, along with the effect of band structure re-normalization [21] is expressed by

$$\varepsilon(\omega) = 1 + \frac{n_0 - n_e}{n_0}\varepsilon_L\left(\omega + \frac{\delta E_g}{\hbar}\right) + \varepsilon_D(\omega) \quad (2)$$

where n_0 is the density of valence electrons [15]. $\varepsilon_L(\omega)$ is the innate dielectric function, δE_g represents the band re-normalization by carrier density, and ε_D is the dielectric function calculated from Drude model [15]. The temperature-dependent optical parameters of silicon are referred to from Ref. [22].

The time-evolution of the temperatures are calculated as:

$$C_{e(h)}\frac{\partial T_{e(h)}}{\partial t} = m_{r,e(h)}\left(\alpha_f I + \beta I^2\right) + E_g \gamma_{e(h)} n_{e(h)} n_{e(h)} n_{h(e)} - \frac{C_{e(h)}}{\tau}\left(T_{e(h)} - T_l\right) - \nabla \cdot \vec{w}_{e(h)} - \frac{\partial n_{e(h)}}{\partial t}\left(m_{r,e(h)} E_g + \frac{3}{2} k_B T_{e(h)} H^{\frac{1}{2}}_{-\frac{1}{2}}\left(\eta_{e(h)}\right)\right) - m_{r,e(h)} n_{e(h)}\left(\frac{\partial E_g}{\partial T_l}\frac{\partial T_l}{\partial t} + \frac{\partial E_g}{\partial n_{e(h)}}\frac{\partial n_{e(h)}}{\partial t}\right) \quad (3)$$

$$C_l\frac{\partial T_l}{\partial t} = -\nabla \cdot (\kappa_l \nabla T_l) + \frac{C_e}{\tau}(T_e - T_l) + \frac{C_h}{\tau}(T_h - T_l) \quad (4)$$

The third and fourth terms in Eq. 3 account for energy loss due to electron-lattice interaction and energy current. The last two terms on the right-hand side include the carrier density changes and band gap energy. Here, $H_\xi^\zeta(\eta) = F_\zeta(\eta)/F_\xi(\eta)$ and $F_\xi(\eta)$ is the Fermi integral. The heat capacities $C_{e(h)}$ are calculated from the carrier densities and temperatures. T_l is calculated following the empirical model, where the term for carrier temperature is replaced by terms for electron and hole temperatures, as described in Eq. 4. Here, κ_l is the thermal conductivity [15].

The propagation of the laser pulse is described by solving Maxwell's equations using FDTD method [15]. Mur's absorbing boundary condition is employed to prevent reflection from the boundary [27].

In our study, the 3TM time step dt is of the order 10^{-1} fs. For FDTD calculation, we define another time step, $dt_m \sim 10^{-3}$ fs, because the time scale of electromagnetic field dynamics is faster than that of electron dynamics. For spatial parameters, the simulation grid size is 150 Å, and the silicon film thickness is varied from 0.01-10 μm, keeping in mind the penetration depth, which is ~10 μm for 775 nm laser. The time-evolution is terminated at 20 ps, which is sufficient time for thermal relaxation between electron, hole, and lattice. We assume a Gaussian pulse of duration 70 fs at full-width half maximum.

Figure 1 shows a schematic depiction of the laser pulse interaction with a silicon film of thickness *d*. Although the

pulse intensity drops exponentially as it travels within the film, there can be a significant reflection from the rear surface of the film if d is small enough. This reflected field interferes with the field within the film, changing the net field.

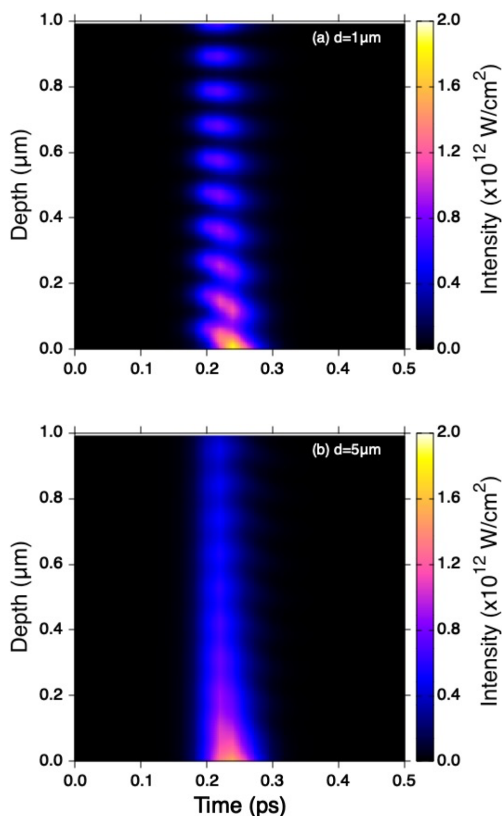

Fig. 2 Spatial-temporal pulse profile inside the silicon film for (a) d = 1 μm and (b) d = 5 μm.

3. Results and discussion

As the thickness is lowered below the penetration depth of ~10 μm, the interference of the laser field reflected from the rear surface with the field within the film becomes significant. Figure 2 shows the typical spatial-temporal profile of the pulse intensity inside the silicon film for (a) d = 1 μm and (b) d = 5 μm. The laser pulse duration is 70 fs, with a wavelength of 775 nm in the vacuum. The fluence is set to 0.18 J/cm^2, which is around the damage threshold of silicon [2]. In Fig. 2(a), the film thickness is small enough to cause interference between the incident field and the field reflected from the rear surface of the film, causing oscillations in the net field in the film. The refractive index of silicon is ~4 at 775 nm, i.e., the wavelength of the pulse inside the film is ~194 nm. The interference occurs with a period of half the wavelength inside the film. Therefore, the period of the oscillations in the pulse profile in Fig. 2 is about 97 nm. As the film thickness approaches the penetration depth for a 775 nm laser (~10 μm), the reflection from the film's rear surface cannot cause significant interference in the field, as shown in Fig. 2(b). The interference seen in the pulse profile in Fig. 2(a) manifests in the electron and lattice dynamics as well, ultimately affecting the damage threshold.

The intensity distribution has peaks and dips as shown in Fig. 2(a). A preferential excitation inside silicon is expected depending on the thickness (d) because the intensity's peak position depends on d. When d is around the multiple of 97 nm (d ~ N×97 nm), constructive interference at the surface may occur. In contrast, destructive interference occurs when d deviates by a quarter of the wavelength from it, i.e., N×97+46.5 nm, because the free end reflection occurs at the rear-surface.

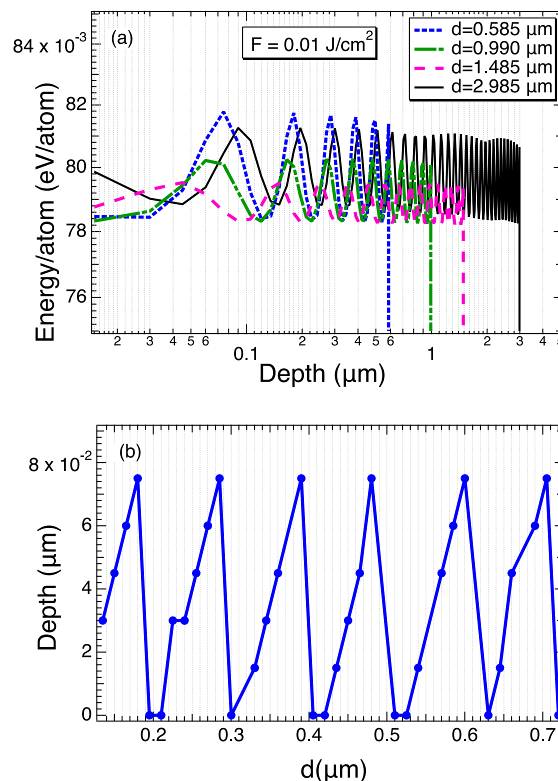

Fig. 3 (a) Variation of total energy with film depth at the last time step for d = 0.585-2.985 μm and fluence 0.01 J/cm^2 and (b) Variation in the position of maximum energy around the front surface with thickness, the fluence is fixed at 0.01 J/cm^2.

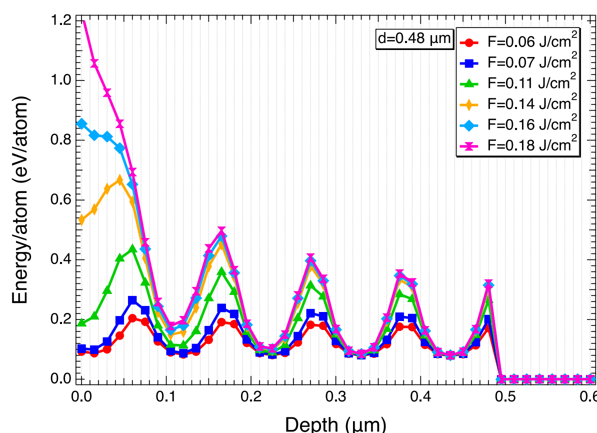

Fig. 4 Spatial variation of absorbed energy density at the last time step for different incident fluence and film thickness 0.48 μm.

Figure 3(a) shows the absorbed energy density as a function of depth for different d. We set the incident fluence at 0.01 J/cm^2. There are many peaks inside the silicon film, which is consistent with the peaks of field intensity. The transmitted field is intense around the surface, while the

reflected field becomes weaker as d increases. As a consequence, the most intense absorption occurs around the front-surface, and excitation inside the film is saturated as d increases. However, as we can see in Fig. 3(a), the interference at the front surface depends on the thickness. At the rear surface, the interference is always constructive. Figure 3(b) shows the highest energy absorption position inside the film as a function of d with the incident fluence of 0.01 J/cm^2. The peak position shows oscillations with an amplitude of 100 nm, due to the interference point being changed by d. This result indicates that thermal damage inside the material occurs with a thin-film target and the damage position depends on the thickness.

The damage position also depends on the peak intensity of the incident laser pulse. Figure 4 shows the intensity dependence of the absorbed energy distribution. As the laser fluence increases, the absorption at the surface is dominant because two-photon absorption becomes the dominant process. The intense two-photon absorption occurring at the surface weakens the transmitted field. As a consequence, the interference effect inside the material becomes a minor effect.

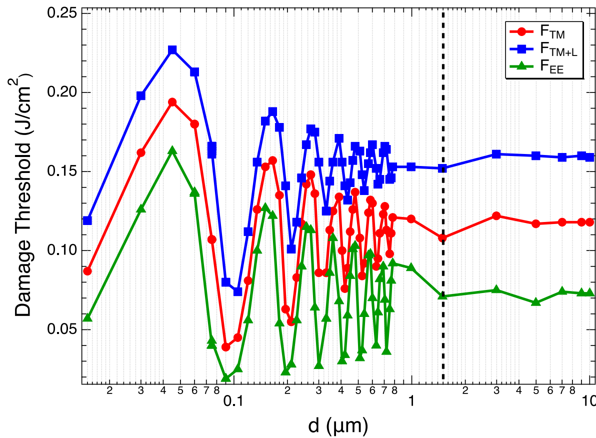

Fig. 5 Calculated thresholds for electron emission (e-emission) (F_{EE}), partial thermal melting (F_{TM}) and complete thermal melting (F_{TM+L}) for d varying from 0.01-10 μm.

In our previous work, we compared the calculated thresholds for possible damage mechanisms [15,16] and compared them with the experimental damage thresholds [2-4,21,28]. Depending on different definitions of damage in experiments, the damage thresholds resembled calculated thresholds for different processes. The definition of damage often depends on the purpose of the experiments, i.e., to avoid or to cause structural modifications. The experimental threshold determined by considering zero damage probability [4] coincided with the calculated thresholds for thermal melting (F_{TM}) and electron-emission (e-emission) (F_{EE}) [15]. However, in ablation experiments, the damage threshold is determined by comparing the diameter of the damaged area with incident pulse intensity, i.e., the damage probability is 100% [2,28]. This threshold coincided with the bond-breaking threshold in the 3TM study [16].

3.1 Thermal melting and e-emission

Figure 5 shows the calculated threshold F_{TM}, F_{TM+L}, and F_{EE} as a function of d at the front surface. Here, F_{TM+L} is the threshold for thermal melting, including latent heat. F_{EE} is calculated as the incident fluence when the average kinetic energy of the electron reaches the work function of silicon (4.65 eV). F_{TM} and F_{TM+L} are calculated as the incident fluence when the melting of the lattice starts and when total latent heat is transferred to the lattice [29], respectively. According to our previous work, F_{TM} and F_{TM+L} coincide with the damage thresholds reported by Allenspacher *et al.* [4] below the pulse duration of 1 ps. The relation of each threshold is always $F_{TM+L} > F_{TM} > F_{EE}$, which is consistent with our previous work for bulk silicon with a pulse duration of 70 fs.

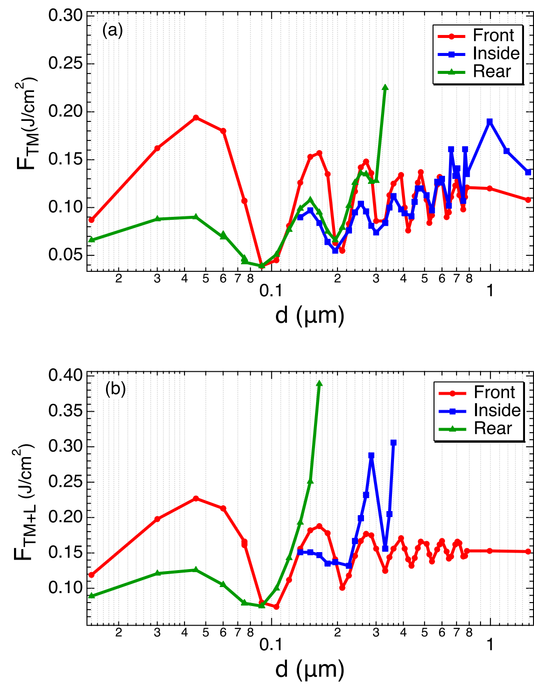

Fig. 6 Comparison of the calculated threshold with varying film thickness on the front surface, inside the film and rear surface for (a) partial melting (F_{TM}) and (b) complete thermal melting (F_{TM+L}).

All thresholds show oscillation with a period of ~100 nm, which indicates that constructive and destructive interference at the front surface affects the damage threshold significantly. The oscillation of thresholds appears up to d = 1.5 μm, which is much smaller than the penetration depth for 775 nm (~10 μm). Since two-photon absorption is the dominant process, the effective penetration depth is significantly reduced for the case of intense laser pulse. All thresholds are independent of d above 1.5 μm, which indicates that we can treat the silicon film thicker than 1.5 μm as a bulk system.

Figures 6(a)-(b) show the calculated F_{TM} and F_{TM+L} for the surfaces and inside the film at the depth of peak dynamics as shown in Fig. 3(b). The thresholds for the rear-surface and inside the film are lower than those for the front surface at small d. As the thickness d increases, thresholds for the rear-surface and inside the film increase because of the longer optical path length and non-linear photo-absorption at the surface.

The thresholds at the rear surface show oscillation in Fig. 6. Since we always observe a constructive interference on the rear surface as shown in Fig.3(a), these results are controversial at the first glance. The oscillation at rear surface may be a result of interference between three components:

transmitted field, field reflected from the rear surface, and field reflected from the front of the film. Since the reflected field from the front surface is small, the oscillation of thresholds at rear surface is weaker than that of the front.

The critical thickness (CT), where the damage at the front-surface occurs first, is an important evaluation index for laser processing. The CTs are 0.51 μm and 0.195 μm for F_{TM}, and F_{TM+L} respectively, inside the film. As the incident laser field increases, the two-photon absorption at the front surface increases, which reduces the transmitted field intensity. As a consequence, the CTs decrease as the damage threshold increases.

3.2 Breaking of bonds

The bond-breaking threshold F_{BB}, is important to understand the laser processing. The comparison of calculated thresholds with ablation experiments in the previous work has shown that F_{BB} is closest to the 100% damage thresholds for silicon [15,16]. The bond-breaking energy (2.3 eV/atom) of silicon is half of the cohesive energy (4.63 eV/atom) [30]. We define the F_{BB} as the fluence at which the absorbed energy density is equal to the bond-breaking energy.

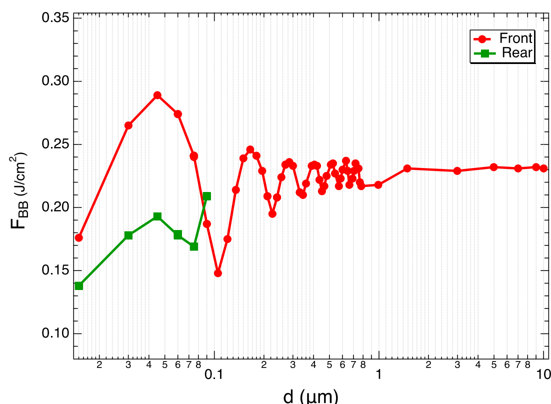

Fig. 7 film thickness dependence of F_{BB} at front and rear surfaces.

Since F_{BB} corresponds to the photo-chemical process, threshold fluence is much higher than other photo-thermal thresholds, F_{TM} and F_{TM+L}. With such intense cases, the excitation inside silicon is not significant. The constructive interference at the rear-surface may still play an important role when the thickness is smaller than the wavelength (< 100 nm). Figure 7 shows the F_{BB} on the front- and rear-surface as a function of *d*. F_{BB} at the front-surface also shows that the oscillations have a period of ~100 nm, up to 1.5 μm. As we expected, the CT is the smallest (~ 0.086 μm) as compared to other thresholds. Thus, damage on the rear surface is possible for very thin films with thicknesses of the order of several tens of nanometers. It should be noted that the thermal process may occur inside, besides the ablation on the surface.

4. Conclusion

We studied the film thickness dependence of laser excitation of silicon thin films using 3TM. We found that the interference of the laser field inside the film plays an important role at relatively lower fluence which induces only thermal processes. The constructive interference at the front- and rear-surfaces reduces the damage threshold. When the destructive interference occurs at the front-surface, thermal damage inside of thin film is dominant with a thickness of 0.2-0.5 μm. The damage threshold with the photo-chemical process by bond-breaking at the rear-surface is lower than that for the front surface when the thickness is smaller than 0.1 μm. This result indicates that the damaged area could change drastically due to interference of the laser field in the material. The interference effect can be seen up to 1.5 μm, which is much smaller than the penetration depth of silicon at 775 nm, ~10 μm because of the two-photon absorption on the surface.

Acknowledgments

This research is supported by MEXT Quantum Leap Flagship Program (MEXT Q-LEAP) under Grant No. JPMXS0118067246. This research is also partially supported by JST-CREST under Grant No. JP-MJCR16N5. The numerical calculations are carried out using the computer facilities of the SGI8600 at Japan Atomic Energy Agency (JAEA).

References

[1] P. P. Pronko, P. A. VanRompay, C. Horvath, F. Loesel, T. Juhasz, X. Liu, and G. Mourou: Phys. Rev. B, 58, (1998) 2387.
[2] J. Bonse, S. Baudach, J. Krüger, W. Kautek, and M. Lenzner: Appl. Phys. A, 74, (2002) 19.
[3] Yusaku Izawa, Yuichi Setuhara, Masaki Hashida, Masayuki Fujita, and Yasukazu Izawa: Jpn. J. Appl. Phys., 45, (2006) 5791.
[4] Paul Allenspacher, Bernd Huettner, and Wolfgang Riede: Proc SPIE, Vol. 4932, (2003) 358.
[5] L. Gallais, D.-B. Douti, M. Commandré, G. Batavičiūtė, E. Pupka, M. Ščiuka, L. Smalakys, V. Sirutkaitis, and A. Melninkaitis: J. Appl. Phys, 117, (2015) 223103.
[6] D. Agassi: J. Appl. Phys., 55, (1984) 4376.
[7] Henry M. van Driel: Phys. Rev. B, 35, (1987) 8166.
[8] K. Sokolowski-Tinten, J. Bialkowski, A. Cavalleri, D. von der Linde, A. Oparin, J. Meyer-ter Vehn, and S. I. Anisimov: Phys. Rev. Lett., 81, (1998) 224.
[9] J.K. Chen, D.Y. Tzou, and J.E. Beraun: Int. J. Heat Mass Transf., 48, (2005) 501.
[10] S. I. Anisimov, B. L. Kapeliovich, and T. L. Perel'Man: J. Exp. Theor. Phys, 39, (1974) 375.
[11] O. Herrfurth, E. Krüger, S. Blaurock, H. Krautscheid, and M. Grundmann: J. Phys. Condens. Matter, 33, (2021) 205701.
[12] T. Terashige, H. Yada, Y. Matsui, T. Miyamoto, N. Kida, and H. Okamoto: Phys. Rev. B, 91, (2015) 241201.
[13] T. Otobe: J. Appl. Phys., 126, (2019) 203101.
[14] E. P Silaeva, A. Vella, N. Sevelin-Radiguet, G. Martel, B. Deconihout, and T. E. Itina: New J. Phys., 14, (2012) 113026.
[15] P. Venkat and T. Otobe: Appl. Phys. Express, 15, (2022) 041008.
[16] P. Venkat and T. Otobe: Appl. Phys. A, 128, (2022) 810.
[17] J. E. Sipe, Jeff F. Young, J. S. Preston, and H. M. van Driel: Phys. Rev. B, 27, (1983) 1141.

[18] Jeff F. Young, J. S. Preston, H. M. van Driel, and J. E. Sipe: Phys. Rev. B, 27, (1983) 1155.
[19] Jing Cui, Aurora Nogales, Tiberio A. Ezquerra, and Esther Rebollar: Appl. Surf. Sci., 394, (2017) 125.
[20] Shunsuke Yamada and Kazuhiro Yabana: Phys. Rev. B, 103, (2021) 155426.
[21] K. Sokolowski-Tinten and D. von der Linde: Phys. Rev. B, 61, (2000) 2643.
[22] Martin A. Green: Sol. Energy Mater. Sol. Cells, 92, (2008) 1305.
[23] Misao Murayama and Takashi Nakayama: Phys. Rev. B, 52, (1995) 4986.
[24] Alan D. Bristow, Nir Rotenberg, and Henry M. van Driel: Appl. Phys. Lett., 90, (2007) 191104.
[25] Hernando Garcia and Ramki Kalyanaraman: J. Phys. B, 39, (2006) 2737.
[26] Brandon J. Furey, Rodrigo M. Barba-Barba, Ramon Carriles, Alan Bernal, Bernardo S. Mendoza, and Michael C. Downer: J. Appl. Phys., 129, (2021) 183109.
[27] Gerrit Mur: IEEE Trans. Electromagn. Compat., EMC-23, (1981) 377.
[28] N. A. Smirnov, S. I. Kudryashov, P. A. Danilov, A. A. Rudenko, A. A. Ionin, and A. A. Nastulyavichus: JETP Letters, 108, (2018) 368.
[29] D. Korfiatis, Kallirroe-Andriane Thoma, and J Vardaxoglou: J. Phys. D: Appl. Phys, 40, (2007) 6803.
[30] Charles Kittel: “Introduction to Solid State Physics”, (Wiley, 8th edition, 2004).

(Received: June 9, 2023, Accepted: November 23, 2023)